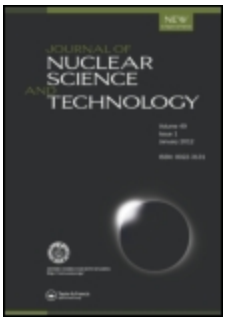

Neutron yield calculation of thin and thick d-D targets by using PHITS with frag data table

Journal:	*Journal of Nuclear Science and Technology*
Manuscript ID	TNST-2021-0179.R1
Manuscript Type:	Technical Material
Date Submitted by the Author:	11-Sep-2021
Complete List of Authors:	Nishitani, Takeo; Nagoya University, Graduated School of Engineering Yoshihashi, Sachiko; Nagoya University, Graduated School of Engineering Ogawa, Kunihiro; National Institute for Fusion Science, Graduate School of Engineering Miwa, Misako; Tohoku University, Graduate School of Engineering Matsuyama, Shigeo; Tohoku University, Graduate School of Engineering Uritani, Akira; Nagoya University, Graduate school of engineering
Keywords:	neutron source, d-D reaction, accelerator, PHITS, frag data, double differential cross-section, gas target
Subject Classification:	209 Neutron Source, Neutron Technology < 2 Radiation, Accelerator and Beam Technologies, 201 Nuclear Physics, Nuclear Reaction for Engineering < 2 Radiation, Accelerator and Beam Technologies, 206 Accelerator and Beam Technology < 2 Radiation, Accelerator and Beam Technologies

SCHOLARONE™
Manuscripts

TECHNICAL MATERIAL

Neutron yield calculation of thin and thick d-D targets by using PHITS with frag data table

Takeo Nishitani[1*], Sachiko Yoshihashi[1], Kunihiro Ogawa[2,3], Misako Miwa[4], Shigeo Matsuyama[4], and Akira Uritani[1]

[1]*Graduate School of Engineering, Nagoya University, Furo-cho, Chikusa-ku, Nagoya 464-8603, Japan;*

[2]*National Institute for Fusion Science, National Institutes of Natural Sciences, 322-6 Oroshi-cho, Toki 509-5292, Japan;*

[3]*SOKENDAI (The Graduate University for Advanced Studies), 322-6 Oroshi-cho, Toki- 509-5292, Japan;*

[4]*Graduate School of Engineering, Tohoku University, 6-6 Aramaki-aza-Aoba, Aoba-ku, Sendai 980-8579, Japan;*

For Peer Review Only

The D(d, n)^{3}He reaction is one of the common monoenergetic neutron sources. We compile the Frag Data table of D(d, n)^{3}He reaction from the literature as an external cross-section data for PHITS. We confirm the validity of the Frag Data table by the calculation of the total and angular neutron yield calculations for an ideal deuterium thin target. Finally, PHITS with the Frag Data table is applied to the angular neutron yield and spectrum calculations of the gas target and the deuterium-loaded titanium target of the Tohoku University Fast Neutron Laboratory.

Keywords: neutron source; d-D reaction; accelerator; PHITS; frag data; double differential cross-section; gas target

*Corresponding author. Email: t-nishitani@energy.nagoya-u.ac.jp

1. Introduction

The D(d, n)^{3}He (d-D) reaction with a Q-value of 3.269 MeV is one of the common monoenergetic neutron sources in the neutron energy range of 1.6-7.7 MeV for the incident deuteron energy less than 4.45 MeV. The generated neutrons are not monoenergetic anymore for the incident deuteron energy higher than 4.45 MeV due to the parasitic deuteron breakup reaction. For the monoenergetic neutron source, a gas target is generally employed as a thin target, where the neutron yield and the angular neutron spectra are easily evaluated by the reaction cross-section including the differential cross-section and the kinematics. Also, the d-D reaction is used as a neutron source of the compact neutron generator, a so-called neutron tube, for many applications such as oil exploration, active neutron interrogation for fissile materials, neutron detector testing, neutron imaging, where a deuterium-loaded metal target is used as a thick target. Generated neutrons are not monoenergetic anymore due to the slowing down effect of the incident deuteron in the target material, where a calculation code is required for the neutron yield evaluation.

The Particle and Heavy Ion Transport code System (PHITS)[1,2] is one of the Monte Carlo particle transport simulation codes not only for neutrons but also charged particles. For the charged particle transport calculation, PHITS uses a nuclear reaction model or a cross-section library such as JENDL-4.0[3] or ENDF/B-VII.1[4]. However, the nuclear reaction model employed in PHITS is not applicable for low energy, typically lower than several MeV/u, and light nucleus. Also, the available ACE format nuclear data library of deuteron-induced reaction is very limited. The ACE format file of the d-D reaction is not available at present. Fortunately, PHITS has a function to read an external cross-section table so-called “Frag Data”. The cross-section of D(d, n)^{3}He reaction itself is well known. We compile the Frag Data table of D(d, n)^{3}He reaction from the literature. Section 2 describes the Frag Data table of D(d, n)^{3}He reaction. As a benchmark, the total neuron yield and the angular neutron yield of an ideal thin deuterium target are discussed in Section 3. The application to the gas target and the deuterium-

For Peer Review Only

loaded titanium target of the Tohoku University Fast Neutron Laboratory (FNL) is described in Sections 4.

2. Frag Data of D(d, n)^{3}He Reaction

The major subject of the Frag Data[5] is the description of the double differential cross-sections (DDX) for a certain reaction. The typical Frag Data table consists of an incident energy table, a reaction cross-section table, an emission particle energy table, an emission angle table, and a DDX table. For the D(d, n)^{3}He reaction, we set the incident deuteron energy to be 0.01-4.5 MeV with 0.01 MeV step. The emission neutron energy is 1.5-8.5 MeV with 0.01 MeV step, and the emission angle is 0-180 degrees with 1-degree step. All those parameters are in the laboratory system (LAB).

The D(d, n)^{3}He reaction cross-section σ_{dD} is well known, and several fitting formulas [6-8] are available. We employed Bosch's formula[8] to calculate the D(d, n)^{3}He reaction cross-section, which is based on the R-matrix analysis and is commonly used in nuclear fusion research. Figure 1 shows the D(d, n)^{3}He reaction cross-section by Bosch's formula and the pointwise data from ENDF/B-VII.1 for the incident deuteron energy from 0.01 to 5 MeV. It is confirmed that the cross-sections by Bosch's formula are in good agreement with the cross-sections from ENDF/B-VII.1.

< Figure 1 >

The DDX, which is a major part of the Frag Data table, is compiled by the combination of the differential cross-section in LAB and the emitted neutron energy calculated by the two-body kinematics. The differential cross-section in the Center-of-Mass system (CM) is represented by the Legendre polynomials as

$$\frac{d\sigma(\Theta)}{d\Omega} = \sigma_{0,CM} \sum_i A_i P_i\,(cos\Theta) \qquad (1)$$

Where $\sigma_{0,CM}$ is the differential cross-section at 0 degrees in CM, P_i is the ith order Legendre function and Θ is the neutron emission angle in CM. The Legendre polynomial coefficient A_i

URL: http://mc.manuscriptcentral.com/tnst E-mail: hensyu@aesj.or.jp
For Peer Review Only

is derived from the table given in the IAEA report [9] by linear interpolation as shown in Figure 2, where the incident deuteron energy is in LAB. Because the D(d, n)^{3}He reaction cross-section is symmetric in CM, all A_i for odd i is 0. In the incident deuteron energy range of 0-5 MeV, A_0, A_2, and A_4 are dominant. A_4 increases with the incident deuteron energy and becomes the most dominant Legendre polynomial coefficient for the incident deuteron energy higher than 3 MeV. Therefore, the differential cross-section in CM has two peaks at 0 degrees and 180 degrees, and the third peak appears at 90 degrees for the incident deuteron energy higher than 3 MeV.

< Figure 2 >

We calculated the differential cross-sections in CM by using the Legendre polynomial coefficient shown in Figure 2 for the incident deuteron energy of 0-4.5 MeV and converted it to the differential cross-sections in LAB. Figure 3 shows the three-dimensional plot of the differential cross-sections in LAB. The peak in the forward direction increases remarkably with the incident deuteron energy. On the other hand, the peak in the backward direction is roll-over. The third peak around 80 degrees is clearly seen for the incident deuteron energy higher than 3 MeV.

< Figure 3>

The differential cross-section is defined as the emitted neutron spectrum at an emission angle for certain incident deuteron energy. Based on the differential cross-sections in LAB and the two-body kinematics, the DDX matrix is created for each incident deuteron energy. In the case of a two-body reaction, the differential cross-section is delta-function-like, which causes a "noisy" or discrete neutron spectrum in PHITS calculations as shown in Figure 4 where DDX matrix with the incident deuteron energy width of 100 keV. The simple interpolation method is adopted in the PHITS calculation using Frag Data. For example, DDX for incident deuteron energy Ed_i and Ed_{i+1} is delta-function-like at En_i and En_{i+1}. We expect that DDX for incident deuteron energy Ed between Ed_i and Ed_{i+1} is also delta-function-like at En between En_i and En_{i+1}. However, PHITS interpolates the DDX by a simple linear combination of DDXs for Ed_i

URL: http://mc.manuscriptcentral.com/tnst E-mail: hensyu@aesj.or.jp
For Peer Review Only

and Ed_{i+1}. The DDX for E_d has two peaks at En_i and En_{i+1}. Therefore, the incident deuteron energy decreases continuously in the deuterium thick target, however, calculated neutron spectra becomes discrete as shown in Figure 4, The improvement of the interpolation method in the PHITS calculation using Frag Data is desired.

< Figure 4>

To avoid the "noisy" neutron spectrum, we should choose the *Ed* bin width (ΔEd) of DDX as narrow as possible under the consideration of total data amount. Here, ΔEd of 20 keV is adopted. Also, we smooth the DDX by the Gaussian function with the standard deviation *STDEV* as

$$STDEV = |E_n(Ed_{i+1},\ \theta_j) - E_n(Ed_i,\ \theta_j)| \quad (2)$$

where $E_n(Ed_i,\ \theta_j)$ is the neutron energy emitted to the angle of θ_j in LAB for the incident deuteron energy of Ed_i. Figure 5 shows the DDX matrix for the incident deuteron energy of 500 keV. In the generated DDX matrix, the neutron emission angle in LAB is from 0 to 180 degrees with one-degree pitch, the emitted neutron energy is from 1.5 to 8.5 MeV with 10 keV pitch, and Ed is from 0.02 to 4.5 MeV with 10 keV pitch. The total amount of the Frag Data table is approximately 230 MB. However, almost all of the differential cross-section matrix is zero except the neutron emission energy at the certain emission angle as shown in Figure 5. According to the new function of PHITS 3.24 or later, we introduced the notation of "0 *-n*" instead of *n+1* consecutive 0s. Finally, the data size is reduced to be 18 MB.

< Figure 5>

3. Benchmark of the Frag Data for Deuterium Thin Target

In order to confirm the validity of the Frag Data, we calculate the total neuron yield and the angular neutron yield of an ideal thin deuterium target with the calculation geometry of PHITS as shown in Figure 6. A pensile deuteron beam bombers an ideal deuterium gas target with a thickness of 10 mm and a pressure of 0.1 atm. The angular neutron yield at the emission

URL: http://mc.manuscriptcentral.com/tnst E-mail: hensyu@aesj.or.jp
For Peer Review Only

angle θ is counted by the belt-shaped tally region with emission angle width of $\Delta\theta$. The total neutron yield is counted by the outer sphere.

< Figure 6>

In the case of the thin target, the total neutron yield Y_n is easily calculated by

$$Y_n = \phi_d \, n_D \, t \, \sigma_{dD} \quad (3)$$

where ϕ_d is the incident deuteron flux, n_D is the deuterium density in the target, and t is the target thickness. Figure 6 shows the total neutron yields per pC of the deuteron beam current calculated by Eq.(3) as a function of the incident deuteron energy and those by PHITS with the Frag Data. We confirmed that the total neutron yields by PHITS agreed well with the theoretical neutron yield. Also, the angular neutron yields $Y_n(\theta)$ are calculated by theory and PHITS, where

$$Y_n(\theta) = \phi_d n_D t \frac{d\sigma(\theta)}{d\Omega} \quad (4)$$

is used for theoretical angular neutron yields. Figure 8 shows the theoretical angular neutron yields and the angular neutron yields by PHITS for the incident deuteron energy of 3 MeV, where is a good agreement.

< Figure 7>

< Figure 8>

The emitted neutron spectrum is calculated by PHITS with a 0.1 MeV energy bin as shown in Figure 9. The energy width is within the energy bin in the forward and backward directions, however, the width is 200-300 keV around 90 degrees, which is mainly due to the emission angle width of the tally shown in Figure 6. The peak energy is plotted against the emission angle compared with the emitted neutron energy calculated by two-body kinematics as shown in Figure 10. Also, PHITS results agree well with the two-body kinematics.

Thus, we confirmed the validity of the PHITS calculation with the Frag Data of D(d, n)^{3}He reaction for the evaluation of the d-D target neutron yield.

< Figure 9>

< Figure 10>

URL: http://mc.manuscriptcentral.com/tnst E-mail: hensyu@aesj.or.jp
For Peer Review Only

4. Application to Deuterium Gas Target and Deuterium-loaded Titanium Target

The Fast Neutron Laboratory (FNL) [10] of Tohoku University is an accelerator-based neutron and ion source facility, where a 4.5 MeV Dynamitron [11] accelerator is employed. FNL has contributed to the neutron cross-section measurements by using several kinds of the target [12]. A deuterium target is one of the most important targets, especially for nuclear fusion research. We applied PHITS with the Frag Data of D(d, n)^{3}He reaction to the evaluation of the neutron yield for the deuterium gas target and the deuterium-loaded titanium target which are used at FNL.

4.1. Deuterium Gas Target of FNL

In Section 3, we treated the ideal gas target. However, a real gas target has a gas cell, a gas inlet tube, and a beam window. Figure 11 shows the schematic view of the FNL gas target. The gas cell is 10.8 mm in diameter and 32 mm in length and has a 6.47 μm thick Havar foil window toward the deuteron beam. Havar is a Cobalt-based alloy and has very high mechanical strength even at high temperatures, which is suitable material for the gas target window. On the neutron yield characterization including angular neutron spectrum, deceleration of the incident beam in the window and the gas itself, and scattering of generated neutrons by the gas cell structure should be taken into account. Therefore, a transport calculation code of charged particles and neutrons such as PHITS is required.

< Figure 11>

The deuteron energy spectra after the Havar foil window are calculated by PHITS for the incident deuteron energy of 2.5, 3.0, 3.5, and 4.0 MeV, where the Coulomb scattering and the energy straggling are taken into account. The energy loss in the window is approximately 0.66, 0.57, 0.52, and 0.47 MeV, respectively. The energy spread is approximately 50 keV of FWHM for all cases. We confirmed that the particle loss by scattering in the window is

URL: http://mc.manuscriptcentral.com/tnst E-mail: hensyu@aesj.or.jp
For Peer Review Only

negligible, which indicates that all deuterons incident to the window reaches the deuterium gas.

In the case of the 3.0 MeV incident deuteron energy with 1 atm deuterium gas target, the angular neutron spectra are shown in Figure 12. We can obtain the quasi monoenergetic neutron as a function of the emission angle as same as the ideal thin target shown in Figure 8. However, the energy width is wider than that in the ideal thin target, which is due to the energy spread of the incident deuteron due to the window and the deuterium gas.

< Figure 12>

For Peer Review Only

4.2. Deuterium-loaded Titanium Target of FNL

A deuterium-loaded titanium thin layer deposited on the copper substrate is widely used as a deuterium thick target. In the high current accelerator typically several mA or higher, the target can be used eternally due to deuterium self-loading. Presently, the beam current of FNL is so low typically ~10 μA, that the deuterium self-loading is not available. Therefore, we have to use a deuterium pre-loaded titanium target. The target should be replaced with a new one frequently because deuterium in the titanium layer reduces by evaporation and consumption. We employed a titanium foil target as shown in Figure 13. The titanium foil of 10 mm in diameter and 0.1 mm in thickness is mounted inside the target shell made of copper. The inner tube pushes the titanium foil to the endplate of the target shell to keep close contact for the heat removal of the foil. The foil can be replaced easily when the amount of deuterium in the foil decreases.

< Figure 13>

Before the experiments, the titanium foils were heated up to 800 °C in a vacuum chamber, and then deuterium gas was introduced into the vacuum chamber. When the temperature decreased gradually to room temperature, the titanium foils absorbed deuterium gas. The amount of deuterium absorbed in each titanium foil was evaluated by the increase of each foil from weight before the absorption. Here, we assumed the deuterium density profile to

be constant in the foil.

Figure 14 shows the angular neutron yield calculated by PHITS with the Frag Data of D(d, n)^{3}He reaction for the deuteron incident energy of 3.0 MeV based on the geometry shown in Figure 13. The atomics density ratio of D/Ti is assumed to be 0.4 which is derived from the weight change of the titanium foil before and after deuterium loading. The range of 3.0 MeV deuteron is approximately 35 μm in the titanium target. Therefore, 3.0 MeV deuterons fully stop in the target. The angular neutron yield decreases with the emission angle. The angular neutron spectra are shown in Figure 15. In the forward direction, the energy spectrum is wider and has a lower energy tail. On the other hand, the energy spectrum at the emission angle larger than 90 degrees is quasi-monoenergetic even in the thick target. In the experiment requiring higher neutron flux such as material irradiation tests, the location of the detector or the material sample should be in the forward direction. The experiment requiring monoenergetic neutrons should use the backward direction. In that case, the gas target is suitable than the thick target.

< Figure 14>

< Figure 15>

5. Conclusion

We compiled the Frag Data table of D(d, n)^{3}He reaction from the literature as an external cross-section data for PHITS. We confirmed the validity of the Frag Data table by the calculation of the total and angular neutron yield calculations for an ideal deuterium thin target. Finally, we calculated the angular neutron yield and spectra of the gas target and the deuterium-loaded titanium target of the Tohoku University FNL. Of course, experimental validation of those target characteristics is desirable. We could not find it in the literature. The experimental validation is future work.

The Frag Data table of D(d, n)^{3}He reaction is useful not only for the d-D target characterization but also for neutron yield estimation at the beam dump of the deuteron

URL: http://mc.manuscriptcentral.com/tnst E-mail: hensyu@aesj.or.jp
For Peer Review Only

accelerator such as a deuteron neutral beam injector (NBI) in the nuclear fusion experiment and IFMIF.

Acknowledgements

The authors wish to thank Prof. T. Sanami of KEK for his technical suggestion on the gas target, and to Prof. Y. Hatano of Toyama University for his contribution to the deuterium gas loading to titanium foils. A part of this work was supported by the LHD cooperated program of KOAH037.

For Peer Review Only

References

[1] Sato T, Iwamoto Y, Hashimoto S, Ogawa T, Furuta T, Abe S, Kai T, Tsai P E, Ratliff HN, Matsuda N, Iwase H, Shigyo N, Sihver L, Niita K: Features of Particle and Heavy Ion Transport code System (PHITS) version 3.02. J Nucl Sci Technol. 2018; 55: 684-690 .

[2] Iwamoto Y, Sato T, Hashimoto S, Ogawa T, Furuta T, Abe S, Kai T, Matsuda N, Hosoyamada R, Niita K: Benchmark study of the recent version of the PHITS code. J Nucl Sci Technol. 2017; 54: 617-635.

[3] Kunieda S, Iwamoto O, Iwamoto N, Minato F, Okamoto T, Sato T, Nakashima H, Iwamoto Y, H. Iwamoto, Kitatani F, Fukahori T, Watanabe Y, Shigyo N, Chiba S, Yamamoto N, Hagiwara M, Niita K, Kosako K, Hirayama S, and Murata T: Overview of JENDL-4.0/HE and benchmark calculations. Proc the 2015 Symposium on Nuclear Data; 2015 Nov19-20; Tokai-mura, Japan: Japan Atomic Energy Agency; 2016, p. 41-46.

[4] Chadwick MB, Herman P, Obložinský M. Dunn ME, Danon Y, Kahler AC, Smith DL, Pritychenko B, Arbanas G, Arcilla R, Brewer R, Brown DA, Capote R, Carlson AD, Cho YS, Derrien H, Guber K, Hale GM, Hoblit S, Holloway S, Johnson TD, T. Kawano T, Kiedrowski BC, Kim H, Kunieda S,1, Larson NM, Leal L, Lestone JP, Little RC, McCutchan EA, MacFarlane RE, MacInnes M, Mattoon CM, McKnight RD, Mughabghab SF, Nobre GPA, Palmiotti G, Palumbo A, Pigni MT, Pronyaev VG, Sayer RO, Sonzogni AA, Summers NC, Talou P, Thompson IJ, Trkov A, Vog RLt, van der Marck SC,Wallner A, White MC, Wiarda D, Young PG: ENDF/B-VII.1 Nuclear Data for Science and Technology: Cross Sections, Covariances, Fission Product Yields and Decay Data, Nuclear Data Sheets. 2011; 112: 2887-2996.

[5] PHITS Ver. 3.24 User's Manual [Internet]. Japan Atomic Energy Agency; [updated 2021 Jun 15; cited 2021 July 20]. Available from: https://phits.jaea.go.jp/manual/manualE-phits.pdf/.

[6] Duan BH: Fusion cross section theory. Battelle Pacific Northwest Laboratory, Richland,

For Peer Review Only

WA; 1972, (BNWL-1685).

[7] Book DL: NRL plasma formulary. Naval Research Laboratory, Washington DC; 1987, (Publication 0084-4040).

[8] Bosch HS, Hale GM: Improved formulas for fusion cross-sections ad reactivities. Nucl Fusion. 1992; 32: 611-631.

[9] Drosg M, Otuka N: Evaluation of the absolute angle-dependent differential neutron production cross sections by the reactions ^{3}H(p,n)^{3}He, ^{1}H(t,n)^{3}He, ^{2}H(d,n)^{3}He, ^{3}H(d,n)^{4}He, and ^{2}H(t,n)^{4}He and of the cross sections of their time- reversed counterparts up to 30 MeV and beyond,Vienna (Austria): International Atomic Energy Agency Nuclear Data Section; 2015. (INDC(AUS)-0019).

[10] Fast Neutron Laboratory [Internet]. Tohoku University; 2021 Jul 28. Available from: http://web.tohoku.ac.jp/fnl/about/whats-fnl/.

[11] Dynamitron E-beam Accelerator [Internet]. IBA; 2021 Jul 28. Available from: https://www.iba-industrial.com/dynamitron-e-beam-accelerator-0/.

[12] Baba M, Tanaka M, Iwasaki T, Matsuyama S. Nakamura T, Ohguchi H, Nakao T, Sanami T, Hirakawa N: Development of monoenergetic neutron calibration fields between 8 keV and 15 MeV, Nucl Instr Meth Phys Res. A. 1996; 376; 888: 115-123.

For Peer Review Only

Figure captions

Figure 1. D(d, n)^{3}He reaction cross-section by Bosch's formula and the pointwise data from ENDF/B-VII.1 for the incident deuteron energy from 0.01 to 5 MeV.

Figure 2. Legendre polynomial coefficient A_i interpolated from the table given in the IAEA report [8].

Figure 3. Three-dimensional plot of the D(d, n)^{3}He differential cross-sections in laboratory system for the incident deuteron energy of 0.01-4.5 MeV.

Figure 4. Neutron energy spectrum of the deuterium-loaded titanium target at 0 degrees for the incident deuteron energy of 3 MeV calculated by PHITS with Frag Data of 100 keV *ΔEd*. The Frag Data is not soothed.

Figure 5. Differential cross-section matrix of D(d, n)^{3}He reaction for the incident deuteron energy of 500 keV.

Figure 6. Schematic view of the calculation geometry of PHITS for the total neuron yield and the angular neutron yield of an ideal thin deuterium target.

Figure 7. The total neutron yields per pC of the deuteron beam for the ideal gas target calculated by the D(d, n)^{3}He reaction cross-section of Bosch's formula and by PHITS.

Figure 8. Angular neutron yields calculated by the differential cross-section derived from the IAEA report [9] and by PHITS for 3.0 MeV deuteron incident to the ideal deuterium gas target of 0.1 atm.

Figure 9. Angular neutron spectrum calculated by PHITS with 0.1 MeV energy bin for 3.0 MeV deuteron incident to the ideal deuterium gas target of 0.1 atm.

Figure 10. Peak energy plotted against the emission angle compared with the emitted neutron energy calculated by two-body kinematics.

Figure 11. Schematic view of the gas target at Tohoku University FNL. The gas cell is 10.8 mm in diameter and 32 mm in length and has a 6.47 μm thick Havar foil window toward the

For Peer Review Only

deuteron beam.

Figure 12. Angular neutron spectra for 3.0 MeV deuteron incident to the FNL gas target with 1 atm deuterium gas pressure.

Figure 13. Schematic view of the deuterium-loaded titanium target for the Tohoku University FNL.

Figure 14. Angular neutron yield calculated by PHITS with the Frag Data of D(d, n)^{3}He reaction for the deuteron incident energy of 3.0 MeV for the deuterium-loaded titanium target for the Tohoku University FNL.

Figure 15. Angular neutron spectra calculated by PHITS with the Frag Data of D(d, n)^{3}He reaction for the deuteron incident energy of 3.0 MeV based on the geometry for the deuterium-loaded titanium target for the Tohoku University FNL.

For Peer Review Only

URL: http://mc.manuscriptcentral.com/tnst E-mail: hensyu@aesj.or.jp

Figure 1. D(d, n)^{3}He reaction cross-section by Bosch's formula and the pointwise data from ENDF/B-VII.1 for the incident deuteron energy from 0.01 to 5 MeV.

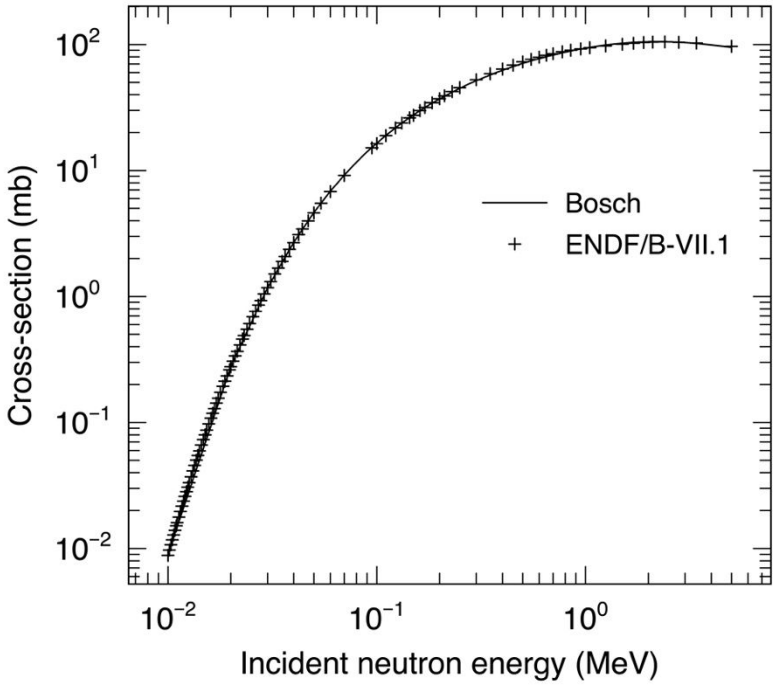

URL: http://mc.manuscriptcentral.com/tnst E-mail: hensyu@aesj.or.jp

Figure 2. Legendre polynomial coefficient A_i interpolated from the table given in the IAEA report [8].

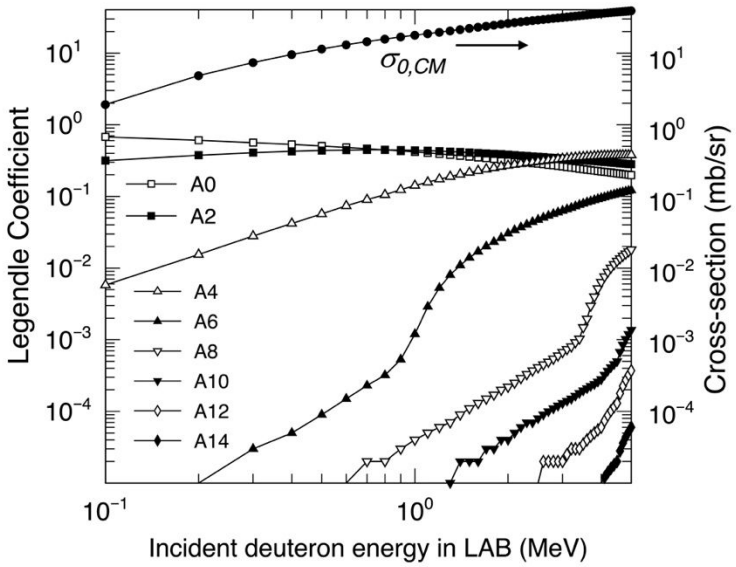

URL: http://mc.manuscriptcentral.com/tnst E-mail: hensyu@aesj.or.jp

Figure 3. Three-dimensional plot of the D(d, n)^{3}He differential cross-sections in laboratory system for the incident deuteron energy of 0.01-4.5 MeV.

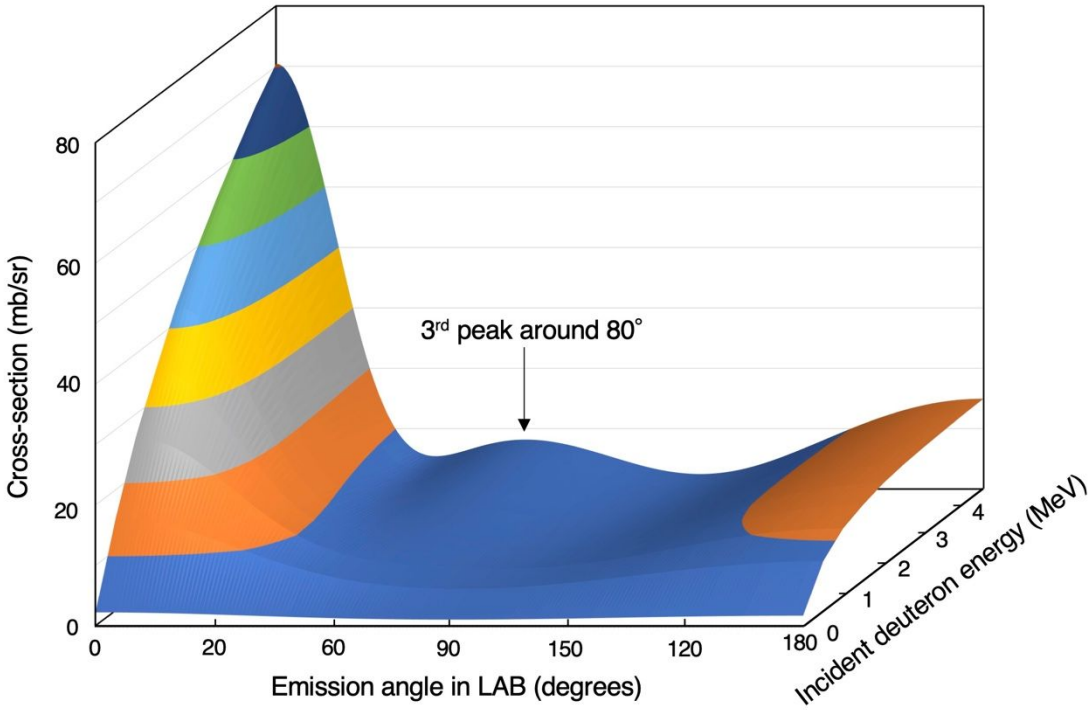

URL: http://mc.manuscriptcentral.com/tnst E-mail: hensyu@aesj.or.jp

Figure 4. Neutron energy spectrum of the deuterium-loaded titanium target at 0 degrees for the incident deuteron energy of 3 MeV calculated by PHITS with Frag Data of 100 keV *ΔEd*. The Frag Data is not soothed.

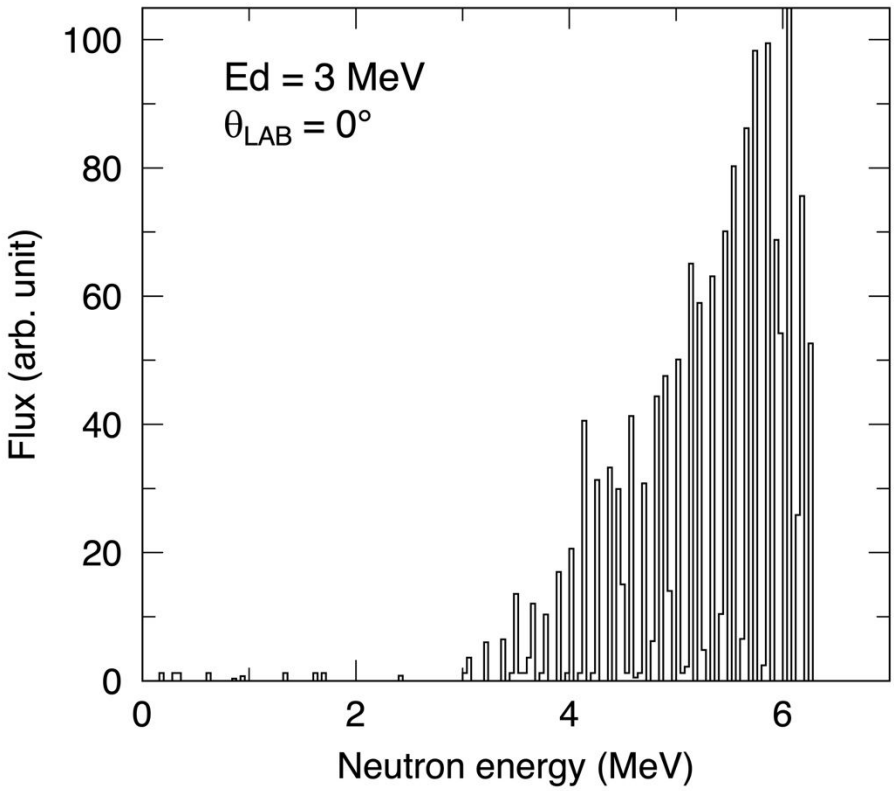

Figure 5. Differential cross-section matrix of D(d, n)^{3}He reaction for the incident deuteron energy of 500 keV.

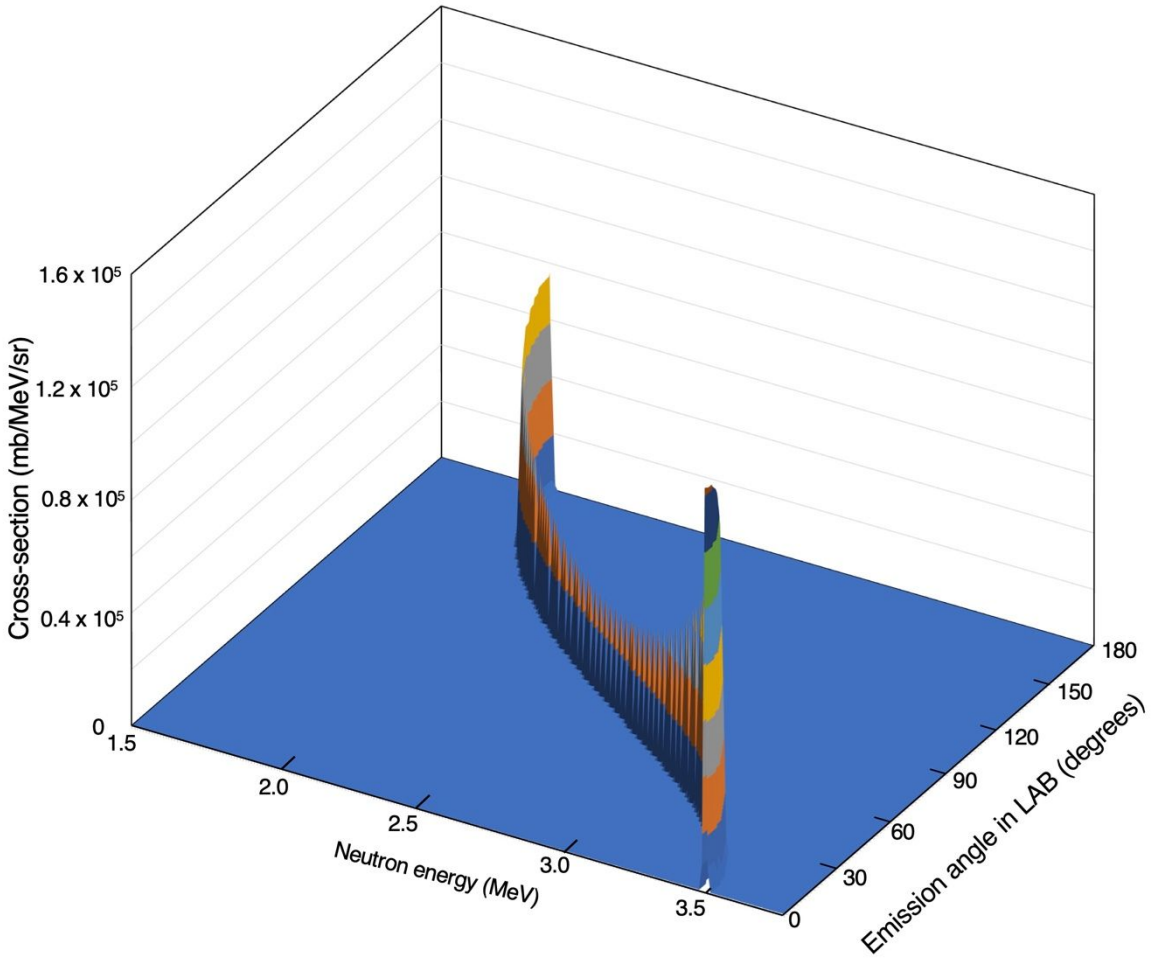

Figure 6. Schematic view of the calculation geometry of PHITS for the total neuron yield and the angular neutron yield of an ideal thin deuterium target.

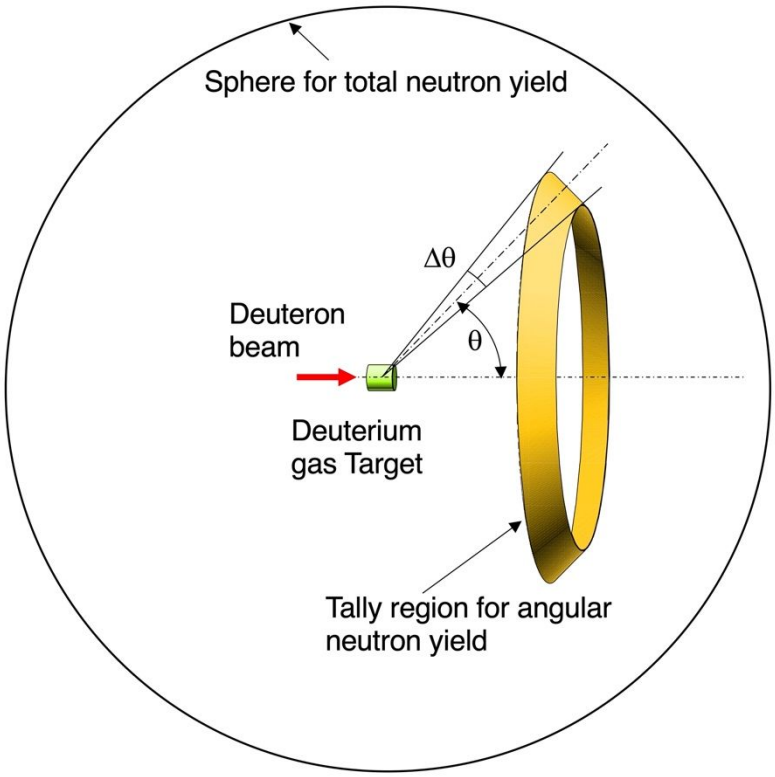

Figure 7. The total neutron yields per pC of the deuteron beam for the ideal gas target calculated by the D(d, n)^{3}He reaction cross-section of Bosch's formula and by PHITS.

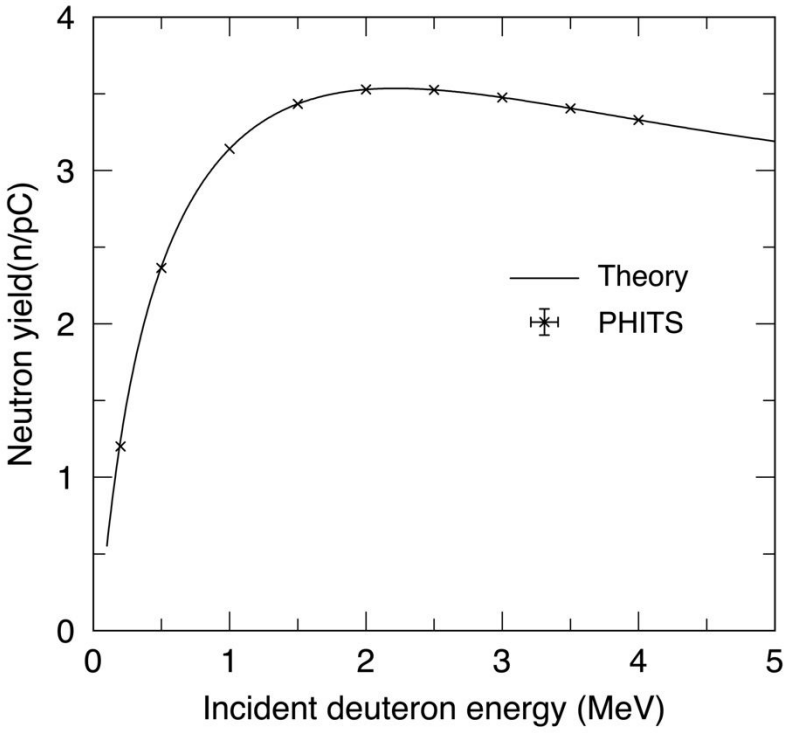

URL: http://mc.manuscriptcentral.com/tnst E-mail: hensyu@aesj.or.jp

Figure 8. Angular neutron yields calculated by the differential cross-section derived from the IAEA report [9] and by PHITS for 3.0 MeV deuteron incident to the ideal deuterium gas target of 0.1 atm.

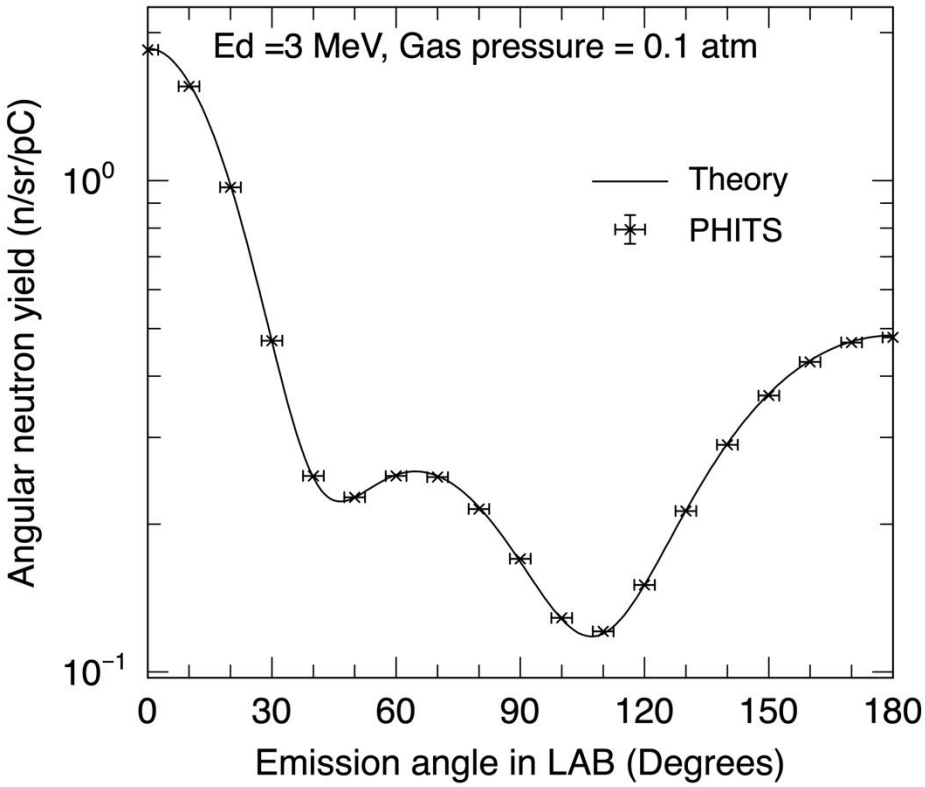

Figure 9. Angular neutron spectrum calculated by PHITS with 0.1 MeV energy bin for 3.0 MeV deuteron incident to the ideal deuterium gas target of 0.1 atm.

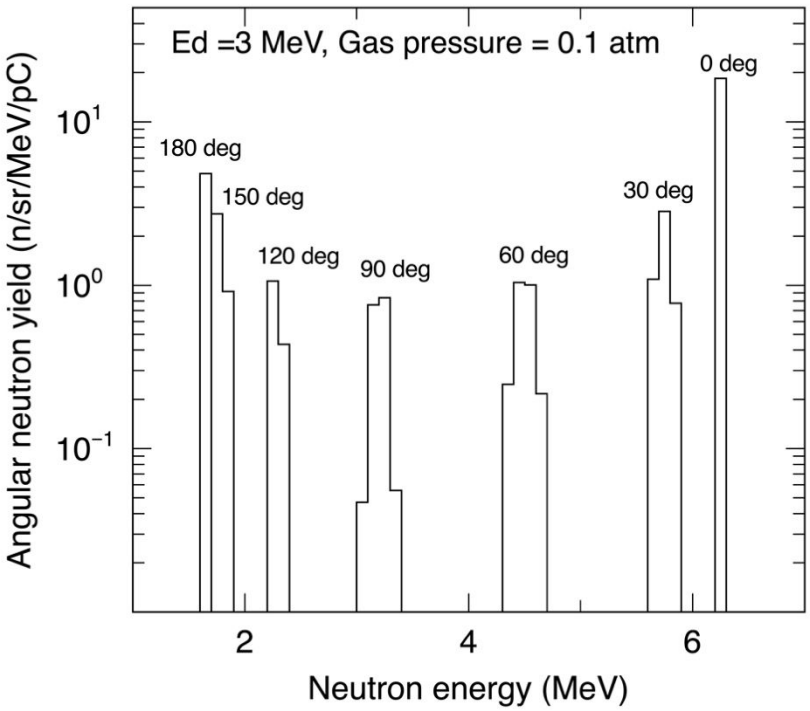

URL: http://mc.manuscriptcentral.com/tnst E-mail: hensyu@aesj.or.jp

Figure 10. Peak energy plotted against the emission angle compared with the emitted neutron energy calculated by two-body kinematics.

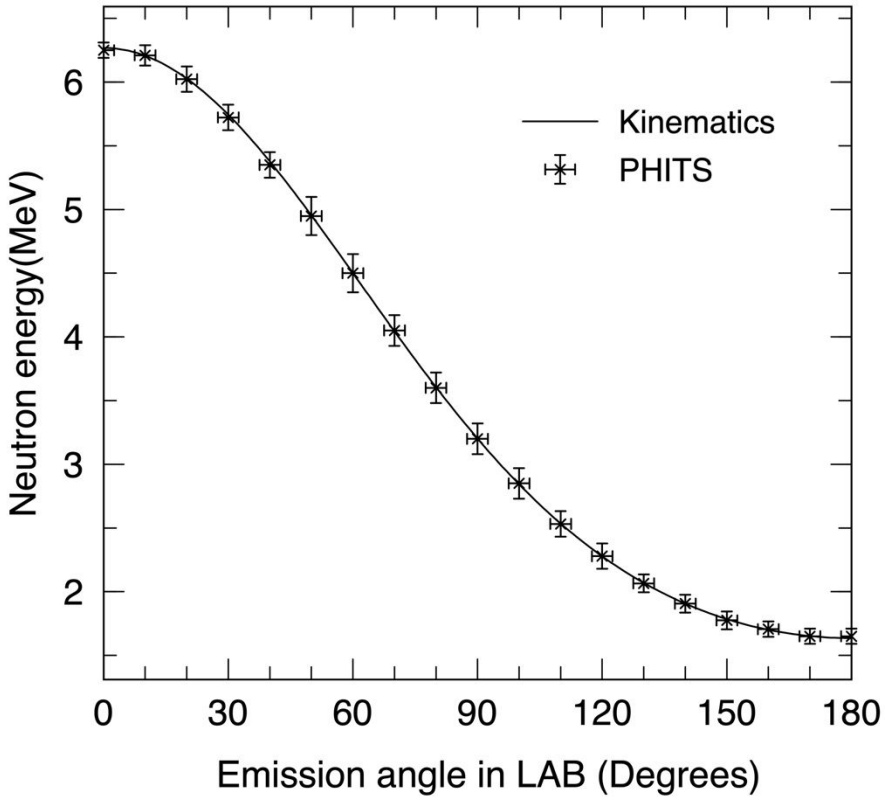

Figure 11. Schematic view of the gas target at Tohoku University FNL. The gas cell is 10.8 mm in diameter and 32 mm in length and has a 6.47 μm thick Havar foil window toward the deuteron beam.

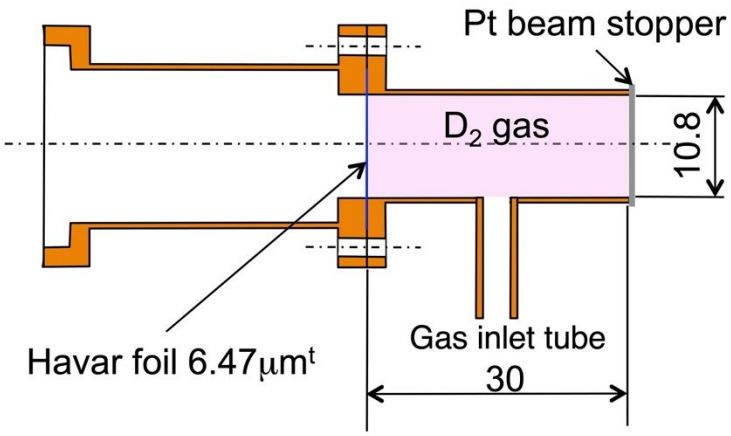

URL: http://mc.manuscriptcentral.com/tnst E-mail: hensyu@aesj.or.jp

Figure 12. Angular neutron spectra for 3.0 MeV deuteron incident to the FNL gas target with 1 atm deuterium gas pressure.

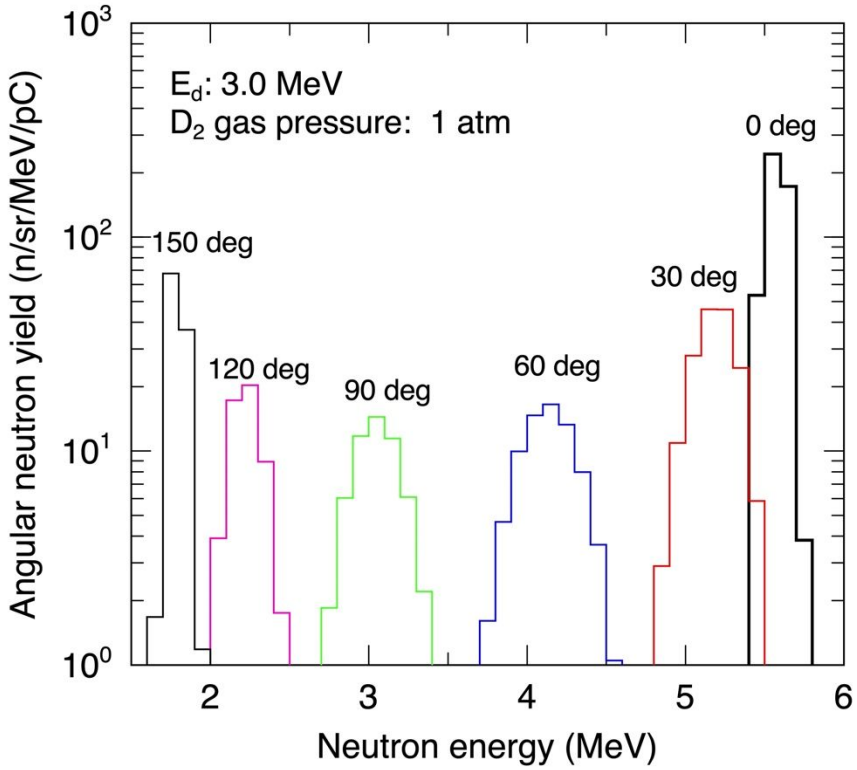

Figure 13. Schematic view of the deuterium-loaded titanium target for the Tohoku University FNL.

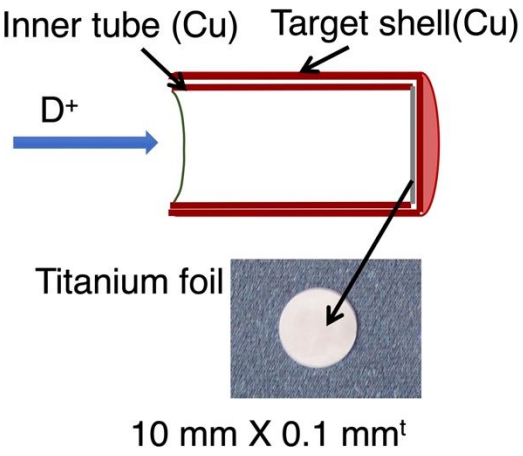

Figure 14. Angular neutron yield calculated by PHITS with the Frag Data of D(d, n)^{3}He reaction for the deuteron incident energy of 3.0 MeV for the deuterium-loaded titanium target for the Tohoku University FNL.

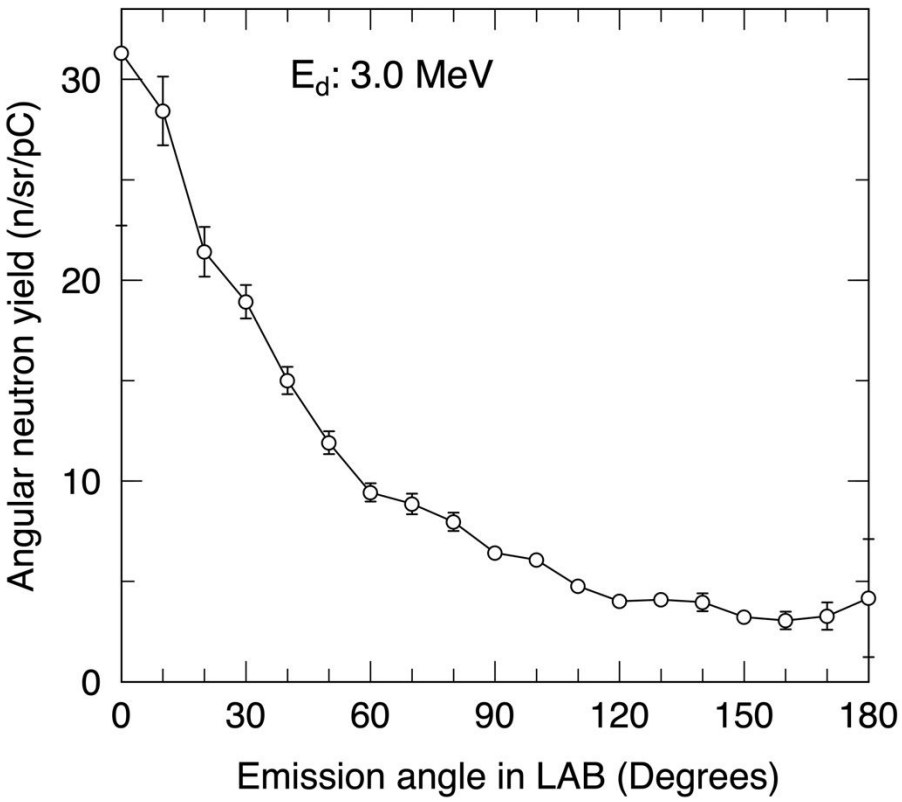

Figure 15. Angular neutron spectra calculated by PHITS with the Frag Data of D(d, n)^{3}He reaction for the deuteron incident energy of 3.0 MeV based on the geometry for the deuterium-loaded titanium target for the Tohoku University FNL.